Eur. Phys. J. B **59**, 291–295 (2007)
DOI: 10.1140/epjb/e2007-00291-3

**The European
Physical Journal B**

Apparent correlations between the static length of relaxation and the linear size of dynamic heterogeneity in fragile liquids

S. Davatolhagh[a]

Department of Physics, College of Sciences, Shiraz University, Shiraz 71454, Iran

Received 1st May 2007 / Received in final form 10 September 2007

Abstract. The most puzzling aspect of the glass transition observed in laboratory is the decoupling of the dynamics from the structure. As an attempt to reconcile the dynamic and the static lengthscales associated with the glass problem, we discuss the apparent correlations between the static relaxation length, defined as that lengthscale over which the potential energy fluctuation is correlated, with the linear size of the dynamic heterogeneity. The dynamic heterogeneous domains with long life-times, may therefore be linked to the droplets of low potential energy, or the tightly bound regions inside the liquid.

PACS. 64.70.Pf Glass transitions

1 Introduction

In the structural glass phenomenology, it is the super-Arrehnius slowing down of the transport properties that is most striking [1]. In particular, the fragile glass-forming liquids are distinguished by a highly temperature-dependent effective energy barrier $E_{\rm eff}(T)$ [2], in their thermally activated expression for the structural or α relaxation time

$$\tau_\alpha(T) = \tau_\infty \exp(E_{\rm eff}(T)/k_{\rm B}T) \qquad (1)$$

where, $\tau_\infty \sim 10^{-13}$ s is a high-T relaxation time, and $k_{\rm B}$ is the Boltzmann constant. The temperature variation of $\tau_\alpha(T)$ for the fragile liquids, is described over a wide range of temperatures by the empirical Vogel-Fulcher (VF) equation [3]:

$$\tau_\alpha(T) = \tau_\infty \exp[DT_0/(T-T_0)] \qquad (2)$$

where, D is a material-specific constant, and the apparent divergence temperature T_0 is called the Vogel-Fulcher temperature, which is often found to be very close to the Kauzmann temperature $T_{\rm K}$ [4] where the configurational entropy of the liquid appears to vanish if it were to stay in equilibrium [5]. We note, however, that equation (2) automatically predicts a phase transition at T_0 [6], as in finite dimensions and short-range interactions a diverging time is normally accompanied by a diverging length. In fact, the very large energy barrier $E_{\rm eff}(T_{\rm g}) \sim 30\ k_{\rm B}T_{\rm g}$ observed for the rather weakly bonded fragile liquids at the laboratory glass temperature $T_{\rm g}$, is regarded as an indication for the cooperative nature of the relaxation dynamics. Several different equilibrium theories of the structural glass transition, invoke an increasing static correlation length that diverges as a power-law $\xi \sim (T-T_{\rm K})^{-\nu}$ at $T_{\rm K} \approx T_0$ [7–9]. However, they do not seem to agree on a common value for the exponent ν (see, Tab. 1). As the dynamics is activated, even a small correlation length can lead to macroscopically large values for $\tau_\alpha(T)$, exceeding the observation time: thus, the falling out of equilibrium of the liquid at the laboratory glass temperature $T_{\rm g} = 1.28 \pm 5.8\%\, T_0$, which is conveniently defined as that temperature where $\tau_\alpha(T_{\rm g}) \approx 10^3$ s [2].

From another perspective, and unlike the simple liquids treated as homogeneous, deeply supercooled liquids also are distinguished by the existence of dynamically heterogeneous domains, typically a few nanometers across, and relaxation times that vary by several orders of magnitude [10,11]. The multi-dimensional nuclear magnetic resonance measurements [10,12], find a dynamic heterogeneity size, $\xi_{\rm het} = 2$–3 nm, or 5 or more atomic diameters near $T_{\rm g}$ for the most fragile of the liquids. The results obtained from a fluctuation theory using the heat capacity spectroscopy data are similar [13], though some times higher [14]. As for their temperature-dependence, more recent experimental procedures have discovered a growing dynamic length accompanying the glass formation in colloidal and molecular liquids [15], and a recent theoretical model suggests a power-law divergence for this strictly dynamical lengthscale at T_0 such that $\xi_{\rm het} \sim (T-T_0)^{-1}$ [16]. Of course, the heterogeneity of time suggests possible heterogeneity in the structure. However, the question of whether the dynamic heterogeneity corresponds to any static correlation in the liquid structure, remains unclear to date. Indeed, a detailed knowledge of the sizes of the static and the dynamic lengthscale, their

---

[a] e-mail: `davatolhagh@physics.susc.ac.ir`

temperature dependencies, and their correlation (if any) can significantly advance our knowledge of the structural glass transition [10].

In a previous work [17], a Bond Ordering (BO) scenario is proposed for a supercooled liquid in which we discuss the correlated relaxation of the bonds (as local configurational energy entities) into low-lying energy states, uncorrelated with the density ordering or crystallization [18,19]. In this bond ordering picture of a supercooled liquid, the structural specific heat C_{s}, arising from the potential energy fluctuation, emerges as the thermal susceptibility associated with the static length for cooperative relaxation of the bonds. This static length of relaxation, ξ_{BO}, is that lengthscale over which the potential energy fluctuation is correlated, and thus defines the typical size of a droplet of low configurational energy inside the system. The scenario predicts a growing (and possibly diverging) C_{s} or ξ_{BO} with the lowering temperature for the fragile liquids, which has been corroborated by the recent Monte Carlo (MC) simulations of a model glass-forming liquid by Fernandez et al. They find that potential energy fluctuation, is correlated over distances much larger than the short range of the interatomic pair interaction in a Binary Mixture of Lennard-Jones (BMLJ) particles [20]. This is made evident by studying the finite-size effects in the equilibrium at the normally inaccessible temperatures using a local swap MC dynamics. Furthermore, the recent isoconfigurational ensemble molecular dynamics simulations have identified droplets of low potential energy in a model water that correlate with dynamic heterogeneities in the form of clusters of low molecular mobility [21]. A molecule in a tightly bound region tends to be less mobile, and the larger the region, the more constrained is the movement of the molecule. In the present paper, we expand on the concept of cooperative bond ordering in order to emphasize the apparent correlations between the static relaxation length, as the average linear size of droplets of low potential energy inside the liquid, and the typical linear size of dynamic heterogeneities with life-times of the order of the structural relaxation time, using some of the most recent results.

The rest of this paper is organized as follows. In Section 2 we recount the implications of a Potential Energy Landscape (PEL) view of the dynamics relevant to our discussion. The main conclusion drawn in that section, paves the way in Section 3 for a phenomenological determination of the structural specific heat C_{s} for the fragile liquids, and ξ_{BO} is determined from C_{s} using an energy version of Fisher scaling law. We also discuss, in Section 3, some important observations with regard to the linear size of dynamic heterogeneity ξ_{het}, and its apparent correlations with the static relaxation length ξ_{BO}. A summary of our main findings appears in Section 4.

2 Lesson from PEL

It is a long held view that in supercooled liquids, the macroscopic dynamics is dominated by the topographic properties of the system's PEL [22,23]: the long-time structural or α relaxation is dictated by thermally activated crossing of the potential energy barriers separating different valleys of the potential energy surface $\Phi(\boldsymbol{r}_1, \ldots, \boldsymbol{r}_N)$, defined over the 3N-dimensional configurational space of the liquid, composed of N atoms. It has been pointed out that activated transport over the potential energy barriers begins to dominate at low temperatures, where $E_{\mathrm{eff}}(T) > 5k_{\mathrm{B}}T$ [22]. This description of the bulk dynamics in terms of the (3N+1)-dimensional PEL, facilitates the study of collective phenomena in viscous liquids [24].

More recently, it has been demonstrated by the molecular dynamics simulations of the BMLJ liquid that the concept of activated hopping between whole superstructures of many PEL minima, called PEL Metabasins (MBs), is central to a quantitative description of the bulk dynamics in a supercooled liquid [25,26]. Here, the time evolution of the system is regarded as a sequence of MB visits each with a residence time τ. The mean residence/escape time from a single MB of energy e is well described by an Arrhenius law $\langle \tau(e,T)\rangle = \tau_\infty \exp(E(e)/k_{\mathrm{B}}T)$, where the MB energy, e, is defined as the energy of the lowest local minimum within the MB. The activation barrier $E(e)$, is found to only depend on the depth of the MB [26,27]: $E(e) \sim -e$. Thus, the lower the e, the higher is the activation barrier $E(e)$. A suitable average over the MBs visited by the system's representative point at a given temperature, thus defines the average residence time $\langle \tau(T)\rangle$ that corresponds to the (super-Arrehnius) α relaxation time:

$$\tau_\infty/\langle \tau(T)\rangle = \int de\, p(e,T) \exp(-E(e)/k_{\mathrm{B}}T) \equiv \exp(-E_{\mathrm{eff}}(T)/k_{\mathrm{B}}T) \qquad (3)$$

where, $p(e,T)\,de$ is the fraction of MBs within the energy range $(e, e{+}de)$ visited by the representative point at T. Clearly, $E_{\mathrm{eff}}(T)$ can be interpreted as an average over the potential energy barriers $E(e) \sim -e$, encountered by the liquid at a given temperature. An spectacular demonstration of this assertion is the concurrence between the crossover to super-Arrehnius relaxation, and the commencement of the variation with the temperature of $\langle e(T)\rangle$ in a molecular dynamics simulation of 80:20 BMLJ model liquid (see, Fig. 1 in [28]). In order to better illustrate the close correlation between $E_{\mathrm{eff}}(T)$ and $\langle e(T)\rangle$, we plot in Figure 1 the dynamic energy barrier $E_{\mathrm{eff}}(T) \equiv k_{\mathrm{B}}T \ln(\tau_\alpha(T)/\tau_\infty)$ against the average value of the PEL minima $\langle e(T)\rangle$, for the temperatures accessed using the data of reference [28]. The units employed are the natural energy units for BMLJ liquid, and data points correspond to those temperatures where the system can be accessed in equilibrium in molecular dynamics simulations. This indicates that, among other things, the effective energy barrier embodied in the VF equation may also be used as an estimate for the temperature variation of $\langle e(T)\rangle$, or that of the average potential energy density of the liquid $\langle \phi\rangle = \langle \Phi\rangle/N$:

$$E_{\mathrm{eff}}(T) \sim -\langle \phi\rangle(T). \qquad (4)$$

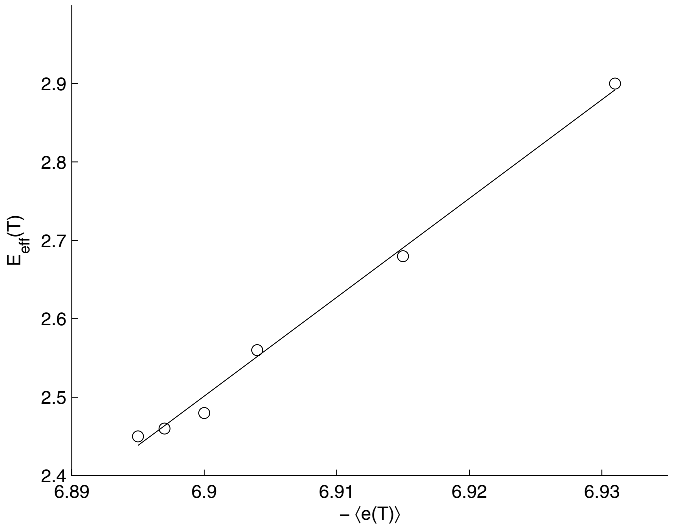

Fig. 1. The dynamical activation energy $E_{\rm eff}(T)$ is plotted against the average depth of the PEL $\langle e(T)\rangle$ for the temperatures accessed using the data of reference [28], in order to illustrate their correlation. Solid line is the least squares fit to the data points.

Table 1. Three different theoretical static lengths at $T_{\rm g}$ for the fragile end of the spectrum, are tabulated for comparison.

Model	ν	$\xi(T_{\rm g})/\xi_\infty$
Bond Ordering [17]	1	7.0
Mean Field [9]	2/3	3.7
Adam–Gibbs [7]	1/3	1.9

There is no doubt that the average potential energy density strongly influences the bulk dynamics of the liquid. It should be pointed out that equation (4) neglects the entropic contributions to free energy barriers. Subsequently, our description of the liquid dynamics in the following section is different from the entropic theories (see also Tab. 1).

3 Cooperative bond ordering

The strong dependence of macroscopic dynamics of a supercooled liquid on its mean potential energy density, as pointed out in Section 2, suggests that the mesoscopic dynamics notably manifested in dynamically heterogeneous domains, may also be linked to droplets of low potential energy inside the liquid. This, and the lack of any discernible two-point density correlations [29], are the main motivating factors for a bond ordering picture of a supercooled liquid in which a central quantity is the *four-point* bond energy correlation function $\langle\phi_{\rm ij}\phi_{\rm lm}\rangle - \langle\phi_{\rm ij}\rangle\langle\phi_{\rm lm}\rangle$, where $\phi_{\rm ij}$ is the short-range pair interaction potential of atoms labeled i and j [17]. By bond ordering, we refer to the correlated relaxation of the bonds (or pair interactions) into low-lying energy states, uncorrelated with the density ordering or crystallization, where the bonds as local configurational energy entities take the place of atoms, as the main statistical objects. The average length over which the bond energy fluctuations are correlated thus defines the static length of cooperative relaxation $\xi_{\rm BO}$, which also sets the lengthscale for the droplets of low potential energy, or the tightly bound regions, inside the liquid.

3.1 Static length of relaxation in fragile liquids

The four-point potential energy density correlation function is defined by

$$G_4(\boldsymbol{r}) \equiv \langle\phi(\boldsymbol{r})\phi(\boldsymbol{0})\rangle - \langle\phi\rangle^2 \tag{5}$$

where, $\phi(\boldsymbol{0})$ is the potential energy of a reference bond at the origin, and $\phi(\boldsymbol{r})$ is that of a bond at the location $\boldsymbol{r}$. The general behavior of the above four-point correlator is given by the Ornstein-Zernick form

$$G_4(r) \sim \exp(-r/\xi_{\rm BO})/r^{d-2+\eta'} \tag{6}$$

where, η' is the power-law decay exponent, d is the space dimension, and $\xi_{\rm BO}$ sets the lengthscale for the exponential decay of the potential energy correlator, or the tightly bound regions inside the system [30]. Furthermore, the thermal susceptibility $C_{\rm s}$ is related to $\xi_{\rm BO}$ via the fluctuation-response equation

$$\begin{aligned} C_{\rm s} &= \frac{1}{k_{\rm B}T^2}\int d^d r G_4(\boldsymbol{r}) \\ &\sim \int^{\xi_{\rm BO}} d^d r/r^{d-2+\eta'} \sim \xi_{\rm BO}^{2-\eta'}. \end{aligned} \tag{7}$$

From equation (7), it is easy to see that η' is related to the power-law increase exponent α of the structural specific heat, and that of the static relaxation length ν, through an energy version of the Fisher scaling law [30]:

$$\alpha = (2-\eta')\nu. \tag{8}$$

By assuming $\eta' = 0$, which is precisely the value obtained from MC simulations of the short-range versions of mean-field structural glass models [32,31], we find the scaling law $\nu = \alpha/2$ for the fragile glass-forming liquids [17]. The structural specific heat $C_{\rm s}$ is the temperature rate of change of the configurational energy $\langle\phi\rangle$. In view of equation (4) for supercooled liquids, it is approximately given by

$$C_{\rm s} = -\left(\frac{\partial E_{\rm eff}}{\partial T}\right)_V. \tag{9}$$

In writing equation (9) the difference between constant pressure and constant volume specific heat is neglected: calculations correspond to a canonical ensemble. Using the effective energy barrier embodied in the VF equation, $E_{\rm eff}(T) = DT_0k_{\rm B}T/(T-T_0)$, we have

$$C_{\rm s} = Dk_{\rm B}T_0^2/(T-T_0)^2. \tag{10}$$

Equation (10) implies a power-law increase for the structural specific heat of the fragile liquids, with an exponent $\alpha = 2$. (It is noteworthy that a critical power-law increase for the structural specific heat has been recently reported in MC simulations of a BMLJ model liquid [20].) We also note that $\nu = \alpha/2 = 1$. Thus, the bond ordering picture predicts the following thermal behavior for $\xi_{\rm BO}$ in the fragile liquids:

$$\xi_{\rm BO}(T) = \xi_\infty T/(T - T_0) \qquad (11)$$

where, ξ_∞ is a high-T or microscopic lengthscale, about the size of an atomic diameter. $\xi_{\rm BO}(T)$ sets the lengthscale for a typical droplet of low configuratinal energy, i.e. a tightly bound region inside the liquid.

3.2 Apparent correlations between $\xi_{\rm BO}$ and $\xi_{\rm het}$

A molecule in a tightly bound region tends to be less mobile, and the larger the region, the more constrained is the molecular movement. In fact, in molecular dynamics simulations of a model liquid water, the droplets of low potential energy are found to be correlated with the dynamic heterogeneities in the form of clusters of low molecular mobility [21]. It is a matter of considerable interest that the predictions of a recent theoretical model for the thermal variation of $\xi_{\rm het}$ (involving a purely dynamic mechanism) is precisely of the same scaling form as of equation (11) for $\xi_{\rm BO}$ [16]. Using the nucleation theory, together with the assumption that the activated processes involve chains/surfaces of molecular displacements, it is predicted that the heterogeneity size must vary as $\xi_{\rm het} \sim (T - T_0)^{-1}$. The theory also is consistent with the observation to the extent that it recovers the VF equation [16]. In Table 1, we compare the values predicted by three different theoretical static lengths at $T_{\rm g}$, for the fragile end of the spectrum using the ratio $T_{\rm g}/T_0 = 1.28 \pm 5.8\%$ [33]. We note that the larger of the three static lengths, $\xi_{\rm BO}(T_{\rm g}) = 7.0$ atomic diameters, is more consistent with the experimentally measured size of heterogeneity, $\xi_{\rm het}(T_{\rm g}) \geq 5$ atomic diameters [10].

As the dynamics is activated, this larger static length may also be used to explain the broad distribution of relaxation times observed for the heterogeneities at $T_{\rm g}$. On comparing equation (11) with the Vogel-Fulcher equation (2), the structural relaxation time of a liquid can be written as

$$\tau_\alpha(T) = \tau_\infty \exp[D\xi_{\rm BO}(T)] \qquad (12)$$

where, $\xi_{\rm BO}(T)$ is measured in units of atomic diameter, and D is of the order of unity for the fragile liquids. This also is the timescale associated with the slowest relaxation mechanism within the liquid. We note that potential energy droplets of all linear sizes $x \leq \xi_{\rm BO}(T)$ do occur inside the liquid with significant probability [34]. In view of equation (12), it is reasonable to assume an activated form $\tau \sim e^{Dx}$ for the mean life-time of a droplet of low potential energy of size $x \leq \xi_{\rm BO}(T)$. Allowing x to vary by a factor of seven in accordance with $\xi_{\rm BO}(T_{\rm g}) = 7.0$, we have τ values that vary by 3 decades. This therefore explains the existence of dynamic heterogeneities near $T_{\rm g}$ whose lifetimes differ by several orders of magnitude [10]. We also see that in the mobile regions the potential energy droplet size x, tends to be rather small, about the size of an atomic diameter. A molecule in this region can move freely unhindered by the neighbors. However, as $x \to \xi_{\rm BO}(T)$, the movement of a typical molecule in the droplet becomes constrained by not only its immediate, but further neighbors as well, as a result of which the molecular mobility is severely reduced over a timescale that is the life-time of the potential energy droplet, $\tau \sim e^{Dx}$. Thus, it is not only the state of bonding of a given molecule, but the size of the potential energy droplet to which it belongs that influence its mobility.

4 Summary

To summarize, the static relaxation length $\xi_{\rm BO}(T_{\rm g})$ is more consistent with the experimentally measured size of dynamic heterogeneity in deeply supercooled fragile liquids. This larger static length may also be used to explain the wide distribution of relaxation times associated with the heterogeneities, which is central to explaining the stretched exponential relaxation and the decoupling of diffusion from viscosity in deeply supercooled liquids. It is a matter of considerable interest that the thermal behavior of $\xi_{\rm BO}(T)$ is precisely of the same form as predicted by a recent dynamical theory for $\xi_{\rm het}(T)$. The above correlations are significant enough to warrant further experimental and simulational investigation into the potential energy droplet picture as a possible physical origin for the dynamic heterogeneities observed in the glass-forming liquids.

References

1. M.D. Ediger, C.A. Angell, S.R. Nagel, J. Phys. Chem. **100**, 13200 (1996); C.A. Angel, Curr. Opin. Solid State Mater. Sci. **1**, 578 (1996); P.G. Debenedetti, *Metastable Liquids* (Princeton University Press, Princeton, 1996)
2. C.A. Angell, J. Non-Cryst. Sol. **131-3**, 13 (1991); **102**, 205 (1988)
3. H. Vogel, Phys. Z. **22**, 645 (1921); G.S. Fulcher, J. Am. Ceram. Soc. **8**, 339 (1925)
4. W. Kauzmann, Chem. Rev. **43**, 219 (1948); F.E. Simon, Z. Anorg. Algemein. Chem. **203**, 217 (1931)
5. C.A. Angell, J. Res. Natl. Inst. Stand. Tech. **102**, 171 (1997); R. Richert, C.A. Angell, J. Chem. Phys. **108**, 9016 (1999)
6. M. Mezard, *First steps in glass theory* in *More is different*, edited by M.P. Ong, R.N. Bhatt (Princeton University Press, Princeton, 2001)
7. G. Adam, J.H. Gibbs, J. Chem. Phys. **43**, 139 (1965)
8. J.H. Gibbs, E.A. DiMarzio, J. Chem. Phys. **28**, 373 (1958)
9. T.R. Kirkpatrick, D. Thirumalai, P.G. Wolynes, Phys. Rev. A **40**, 1045 (1989)
10. M.D. Ediger, Annu. Rev. Phys. Chem. **51**, 99 (2000)
11. H. Sillescu, J. Non-Cryst. Solids **243**, 81 (1999)
12. U. Tracht, M. Wilhelm, A. Heuer, H. Fang, K. Schmidt-Rohr, H.W. Spiess, Phys. Rev. Lett. **81**, 2727 (1998)
13. E. Donth, J. Non-Cryst. Solids **53**, 325 (1982)

14. E. Donth, H. Huth, M. Beiner, J. Phys.: Condens. Matter **13**, 451 (2001)
15. L. Berthier, G. Biroli, J.-P. Bouchaud, L. Cipelletti, D. ElMasri, D. L'Hote, F. Ladieu, M. Pierno, Science **310**, 1797 (2005)
16. J.S. Langer, Phys. Rev. Lett. **97**, 115704 (2006); Phys. Rev. E **73**, 041504 (2006)
17. S. Davatolhagh, J. Phys.: Condens. Matter **17**, 1275 (2005)
18. H. Tanaka, J. Phys.: Condens. Matter **10**, L207 (1998); H. Tanaka, J. Phys.: Condens. Matter **11**, L159 (1999)
19. See also, H. Tanaka, J. Chem. Phys. **111**, 3163 (1999); H. Tanaka, J. Chem. Phys. **111**, 3175 (1999)
20. L.A. Fernandez, V. Martin-Mayor, P. Verrocchio, Phys. Rev. E **73**, 020501 (2006)
21. G.S. Matharoo, M.S. Gulam Razul, P.H. Poole, Phys. Rev. E **74**, 050502 (2006)
22. M. Goldstein, J. Chem. Phys. **51**, 3728 (1969)
23. F.H. Stillinger, T.A. Weber, Phys. Rev. A **25**, 978 (1982); Science **225**, 983 (1984)
24. F.H. Stillinger, Science **267**, 1935 (1995)
25. S. Buchner, A. Heuer, Phys. Rev. Lett. **84**, 2168 (2000); Phys. Rev. E **60**, 6507 (1999)
26. B. Doliwa, A. Heuer, Phys. Rev. Lett. **91**, 235501 (2003); Phys. Rev. E **67**, 031506 (2003)
27. A. Saksaengwijit, B. Doliwa, A. Heuer, J. Phys.: Condens. Matter **15**, 1237 (2003)
28. S. Sastry, P.G. Debenedetti, F.H. Stillinger, T.B. Schroder, J.C. Dyre, S.C. Glotzer, Physica A **270**, 301 (1999)
29. R.L. Leheny, N. Menon, S.R. Nagel, D.L. Price, K. Suzuya, P. Thiyagarajan, J. Chem. Phys. **105**, 7783 (1996); A. van Blaaderen, P. Wiltzius, Science **270**, 1177 (1995)
30. See, e.g., S. Davatolhagh, Am. J. Phys. **74**, 441 (2006)
31. A. de Candia, A. Coniglio, Phys. Rev. E **65**, 16132 (2001)
32. See, also, Fig. 3 in M. Campellone, B. Coluzzi, G. Parisi, Phys. Rev. B **58**, 12081 (1998)
33. U. Mohanty, J. Chem. Phys. **100**, 5905 (1994); Adv. Chem. Phys. **89**, 89 (1994); A.B. Bestul, S.S. Chang, J. Chem. Phys. **40**, 731 (1964)
34. An analogous, but long-range effect, arising from two-point density fluctuations is the cause of critical opalescence observed in fluids at their critical point. See, e.g., H.E. Stanley, *Introduction to phase transitions and critical phenomena* (Oxford University Press, Oxford, 1971)